# 15

# Dispersion Surfaces

## CHAPTER PREVIEW

The analysis of Bloch waves given in the previous chapter is closely related to the classic analysis of waves that you've seen in condensed-matter physics or semiconductor theory. In semiconductors in particular, we often talk of band diagrams and indirect or direct band gaps. We use terms like conduction bands, valence bands, and Brillouin-zone boundaries (BZBs). We visualize these quantities by drawing diagrams of $E(\mathbf{k})$, the electron energy (which is a function of **k)** versus **k**, the wave vector. This plot of $E(\mathbf{k})$ versus **k** is known as a dispersion diagram. To remind you of the magnitudes involved, the band gap in Si is 1.1 eV and that of Ge is 0.7 eV. In a good insulator, it can be 10 eV. We now follow the same approach to represent pictorially what we described in equations in Chapters 13 and 14. Remember that the big difference from the solid-state physics approach is that the energy of the electrons in the beam in the TEM is $\geq$100 keV.

In this chapter we will see the real origin of the extinction distance $\xi_{\mathbf{g}}$, which we introduced in equation 13.4. We will discuss how it relates to particular materials and why it varies with the diffraction vector being used. We will then discuss the physical origin of the concept of the effective extinction distance: i.e., the value which the extinction distance appears to have when $s \neq 0$. This discussion of dispersion surfaces is included as a separate chapter, so that you can omit it without affecting your understanding of the rest of the text. We should give you a warning: this is a subject which has probably turned off many potential microscopists. It can be very mathematical, pure theoretical physics, or it can provide many useful insights into image formation. We are trying for the latter. If we aren't completely successful, take heart; nearly every established microscopist has survived without completely mastering this concept!

## 15.1 INTRODUCTION

The analysis of Bloch waves as they apply to electrons in solids is well documented in the condensed-matter physics literature. However, what we want from the theory is different from what an electrical engineer might want: we want to understand how it applies to the formation of contrast in TEM images and DPs. With this aim in mind, we will again follow the treatment given in Metherell's classic and well-hidden article, already referenced in Chapters 13 and 14. In Chapter 14, we derived equations relating **k** to $U_{\mathbf{g}}$. (See Section 14.2 for the definition of $U_{\mathbf{g}}$.) Specifically, we found that there are two Bloch waves if there are two Bragg beams, **0** and **g**. We can rewrite equation 14.35 incorporating equation 14.32 as

$$\frac{C_{\mathbf{g}}^{(j)}}{C_{\mathbf{0}}^{(j)}} = \frac{\left(\mathbf{k}^{(j)}\right)^2 - K^2}{U_{-\mathbf{g}}} = \frac{U_{\mathbf{g}}}{\left(\mathbf{k}^{(j)} + \mathbf{g}\right)^2 - K^2} \qquad (15.1)$$

where $C_{\mathbf{0}}^{(j)}$ is the amplitude of the plane wave with wave vector $\mathbf{k}^{(j)}$, and $C_{\mathbf{g}}^{(j)}$ is the amplitude of the plane wave with wave vector $\mathbf{k}^{(j)} + \mathbf{g}$. The Bloch wave was given in equation 14.12 as

$$b^{(j)}(\mathbf{r}) = \sum_{\mathbf{g}} C_{\mathbf{g}}^{(j)} e^{2\pi i\left(\mathbf{k}^{(j)}+\mathbf{g}\right)\cdot\mathbf{r}} \qquad (15.2)$$

Equation 15.1 says that the values of $C_{\mathbf{g}}^{(j)}$ and $C_{\mathbf{0}}^{(j)}$ are directly related to $k^{(j)2}$–$K^2$ and thus to $k^{(j)}$–$K$.

In the general many-beam case (actually, in any situation where we have more than two beams), the situation is more complicated. However, we can separate the problem into two parts

- Determine all the allowed wave vectors $\mathbf{k}^{(j)}$ in a crystal, including all possible orientations of the crystal.
- Determine which set of the allowed $\mathbf{k}^{(j)}$ wave vectors is actually present when you fix the orientation of your crystal.

The first statement fixes the total energy of the electron and selects the crystal. The second statement applies the boundary conditions for the particular situation you are considering, as we'll illustrate in Sections 15.5 and 15.6.

The solution to the first part of the problem is found by setting $|\mathcal{A}^{(j)}| = 0$. (We defined $\mathcal{A}^{(j)}$ in Section 14.3 and gave an expression for it in Section 14.5.) If you multiply the determinant, you get a polynomial to the power $2n$ in $\mathbf{k}^{(j)}$

$$\mathcal{A}_{2n}\left(\mathbf{k}^{(j)}\right)^{2n} + \mathcal{A}_{2n-1}\left(\mathbf{k}^{(j)}\right)^{2n-1} + \mathbf{K} = 0 \qquad (15.3)$$

The coefficient $\mathcal{A}_n$ depends on $\mathrm{K}^2$ (i.e., the energy) and $\mathbf{g}$ (i.e., the crystal).

So, the polynomial in $\mathbf{k}^{(j)}$ relates $\mathbf{k}^{(j)}$ to the total energy. This is a dispersion relation as we defined the term in Section 14.4. The equation has $2n$ roots and some might be complex. To quote Metherell, "at first sight therefore, the situation appears to be a complicated one!" So in following Metherell we make two simplifications

- We consider only the high-energy case.
- We assume that we only excite reflections in the ZOLZ.

There are three reasons for reminding you of these simplifications

- If you want to make a Bloch-wave calculation where you include more than two Bragg beams, then you will need a computer.
- The diagrams we're considering in this chapter are a pictorial representation. The diagrams help us think about what is actually happening to the Bloch waves. If we just did the calculation, we would lose the physical 'feel' for the problem.
- None of the diagrams we will draw will consider HOLZ reflections; if we make the beam energy high enough, we don't need to consider them. However, the energy is not really that high and HOLZ reflections are not only seen experimentally, but can also provide valuable information, as we'll see in Chapters 20 and 21. The saving factor is that modern computers have no problems in handling these equations, especially since they are so amenable to matrix manipulation.

**THE DISPERSION SURFACE**
. . .is a pictorial representation of the relationship between **k** and energy.

## 15.2 THE DISPERSION DIAGRAM WHEN $U_g = 0$

We start with equation 14.34, namely

$$\left(\left|\mathbf{k}^{(j)}\right| - K\right)\left(\left|\mathbf{k}^{(j)} + \mathbf{g}\right| - K\right) = \frac{|U_g|^2}{4K^2} \qquad (15.4)$$

Remember that this equation was derived for the two-beam case. When the electrons are in the vacuum, i.e., outside the specimen, the Fourier coefficients $U_g$ are 0. When $U_g = 0$, the left side of this equation is zero and the equation has two solutions.

$$K = \left|\mathbf{k}^{(j)}\right| \text{ or } K = \left|\mathbf{k}^{(j)} + \mathbf{g}\right| \qquad (15.5)$$

where $j$ is 1 or 2. If we plot out these two solutions we find, as shown in Figure 15.1, that we have two interpenetrating spheres, since both $\mathbf{k}_I$ and $\mathbf{k}_D$ can lie in any direction. Since these two **k** vectors have the same length, the two spheres represent surfaces of constant energy, called dispersion surfaces, one centered on O and the other centered on G.

Of course, we already know that the energy of the electron in a vacuum is related to its wave vector by

$$E = \frac{p^2}{2m} = \frac{\mathrm{h}^2\chi^2}{2m} \qquad (15.6)$$

where **p**, the momentum, is related to the wave vector in a vacuum, $\boldsymbol{\chi}$, by $\mathbf{p} = \mathrm{h}\boldsymbol{\chi}$. Here, $\boldsymbol{\chi}$ is the **K** when the electron is in a vacuum.

Rearranging, we have

$$\chi = \left\{\frac{2m}{\mathrm{h}^2}E\right\}^{\frac{1}{2}} \qquad (15.7)$$

The dotted line drawn in Figure 15.1 represents a plane that is defined by the circle created by the intersecting spheres. You will probably be very familiar with the BZB from condensed-matter physics.

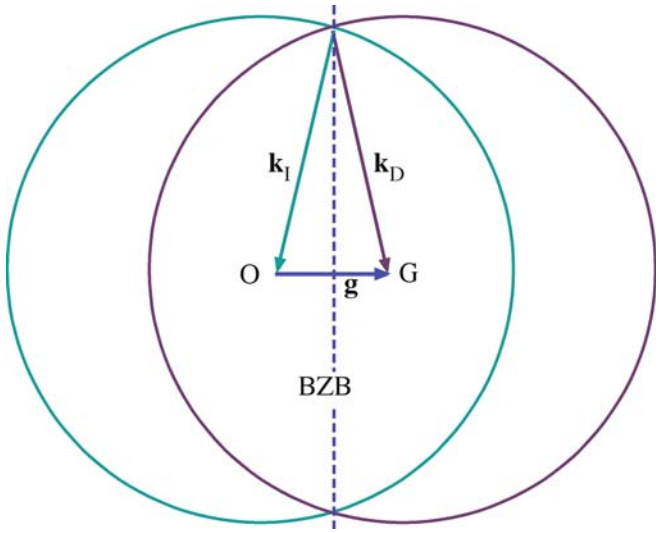


**FIGURE 15.1.** Cross section through two spheres of radii $\mathbf{k}_I$ and $\mathbf{k}_D$ centered on O and G, respectively. The spheres represent surfaces of constant energy and the dotted line is the trace of the diffracting plane (and is also equivalent to the BZB).

While you work through the diagrams in this chapter, you must remember that for high-energy electrons the scattering angles, e.g., $2\theta_B$, are usually small and the region of interest in reciprocal space is, therefore, close to the BZB. We can redraw part of Figure 15.1 to show an enlarged view of the region close to the BZB in Figure 15.2. At high energies, we approximate the surfaces as a pair of straight lines because $\lambda$ is very small.

## 15.3 THE DISPERSION DIAGRAM WHEN $U_g \neq 0$

When $U_g \neq 0$ we know from equation 15.4 that $K$ can never be equal to $|\mathbf{k}_I|$ or $|\mathbf{k}_D|$. Since equation 15.4 is quadratic we must have two values for $|\mathbf{k}|$. So, the two 'spheres' can't intersect if $U_g \neq 0$. You noticed that equation 15.4 *resembles* that for a hyperbola, $xy = a$, where the $x$ and the $y$ axes are shown in Figure 15.2. We can draw these two hyperbolae with their asymptotes as shown in Figure 15.3. These surfaces (remember we are in three dimensions) are known as *branches* of the dispersion surface. The upper branch (identified here by the '1') corresponds to $\mathbf{k}^{(1)}$ and the lower (identified by the '2') to $\mathbf{k}^{(2)}$. We now have vectors $\mathbf{k}^{(1)}$ and $\mathbf{k}^{(2)}$ where we used to just have $\mathbf{K}_I$. There are some critical points to remember in this discussion from Chapters 13 and 14

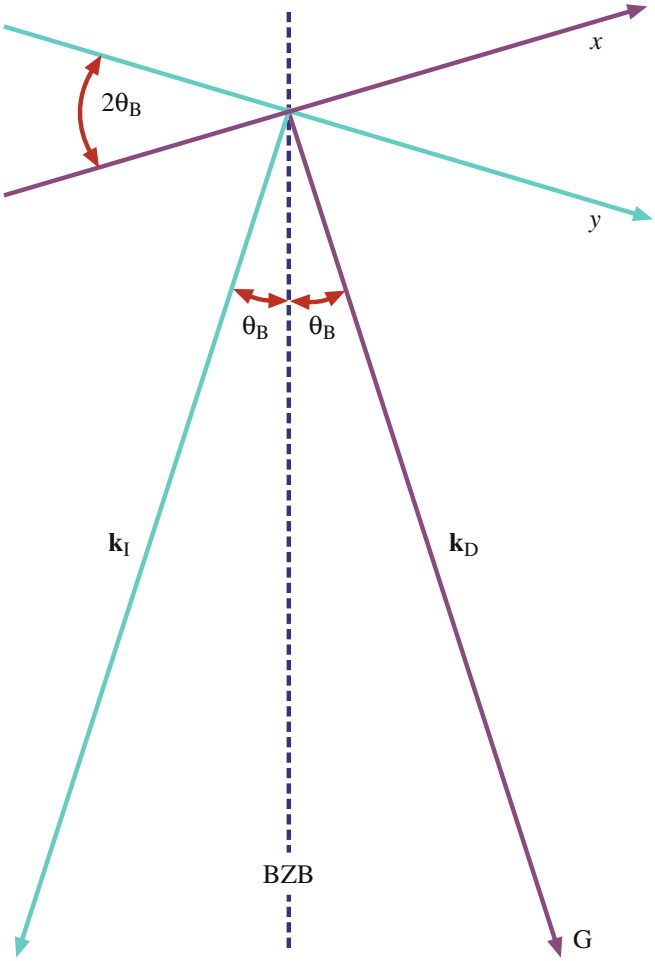


**FIGURE 15.2.** An enlarged view of the interception of the two dispersion spheres at the BZB. The projections of the two dispersion surfaces approximate to straight lines $x$ and $y$ which are normal to $\mathbf{k}_D$ and $\mathbf{k}_I$, respectively.

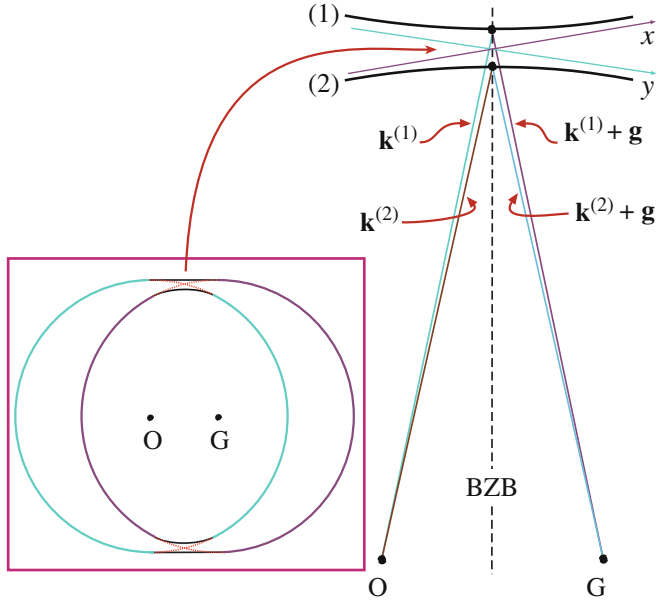


**FIGURE 15.3.** When the electron is inside the specimen (i.e., $U_g \neq 0$) there are two values of $\mathbf{k}$. The two dispersion spheres can't intersect and two branches of the dispersion surface (1) and (2) are created. The enlarged view of the 'non-intersection' shows the vectors, $\mathbf{k}^{(1)}$ and $\mathbf{k}^{(2)}$, and $\mathbf{k}^{(1)} + \mathbf{g}$ and $\mathbf{k}^{(2)} + \mathbf{g}$.

- The Bloch wave $b^{(1)}(\mathbf{k}^{(1)}, \mathbf{r})$ is associated with $\mathbf{k}^{(1)}$.
- The Bloch wave $b^{(2)}(\mathbf{k}^{(2)}, \mathbf{r})$ is associated with $\mathbf{k}^{(2)}$.
- The intensity of the Bragg beam is a function of thickness $|\phi_g(t)|^2 \propto \sin^2(\pi t \Delta k)$ (from equation 13.45).

The difference between Figures 15.1 and 15.3 is the gap between the two branches in Figure 15.3. This gap is present because $U_g$ is not zero; $U_g$ is not zero because we have a periodic array of atoms, i.e., a crystal. This gap is directly analogous to the band gap in semiconductor theory where there are forbidden electron energies within the crystal.

## 15.4 RELATING DISPERSION SURFACES AND DIFFRACTION PATTERNS

We can gain a lot of physical insight into Bloch waves using the dispersion-surface construction rather than solving the Bloch-wave equations on the computer. Our approach is relatively simple.

- We start with the dispersion surface shown in Figure 15.4A and draw an initial line to represent the incoming beam traversing the thin foil. We assume an idealized thin specimen with parallel surfaces that are perpendicular to the vertical, optic axis of our TEM and we choose **g** to be parallel to the surface. The incident beam is allowed to be inclined to the surface of the specimen.
- We then draw a line normal to any surface that the initial line encounters. This allows us to match the components of wave vectors parallel to that surface. This is the wave-matching construction.

**WAVE MATCHING**
If we were doing this mathematically, this matching would be the boundary condition.

- We then extend the points $M_1$ and $M_2$ back to the '**k**' spheres in Figure 15.4B; these spheres are the **χ** spheres when we are in the crystal.
- The last part of the process is always to relate the waves in the crystal to the beams in the vacuum since our recording film, CCD camera, etc., is always outside the crystal.

That's the plan—now we go through it step by step. As shown on the enlarged view in Figure 15.5, each of the **k** vectors has an associated wave amplitude $C_{\mathbf{g}}^{(j)}$ associated with it.

In this discussion, we will limit ourselves to the two beams, O and G. As we know from Section 13.8, the only values of $C$ (the coefficients of the Bloch waves) that will then be non-zero are $C_{\mathbf{0}}^{(1)}$, $C_{\mathbf{0}}^{(2)}$, $C_{\mathbf{g}}^{(1)}$, and $C_{\mathbf{g}}^{(2)}$.

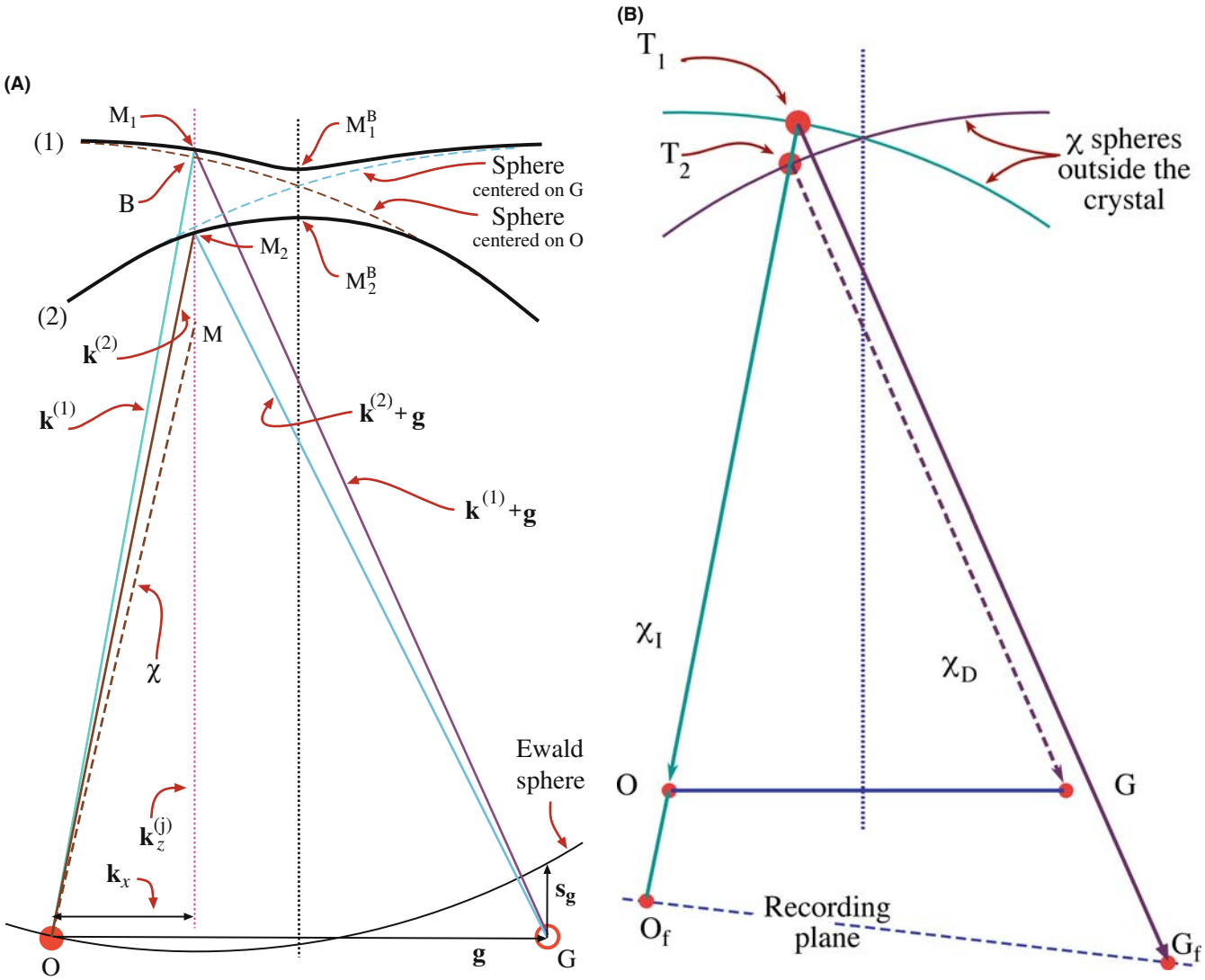


**FIGURE 15.4.** (A) Combination of the dispersion surfaces (1) and (2), centered on O and G, with the Ewald sphere construction. The surface of the specimen has been set to be parallel to **g**, so points $M_1{}^B$ and $M_2{}^B$ on the branches (1) and (2) are excited. The incident beam direction is then parallel given by the vector **MO**. If we tilt the beam so χ (as shown) becomes more vertical, the excited points move to $M_1$ and $M_2$ giving the tie line $M_1M_2$. The vectors $\mathbf{k}^{(1)}$ and $\mathbf{k}^{(2)}$ start at $M_1$ and $M_2$, respectively, and end on O. (B) Extension of the lines $OM_1$ and $OM_2$ in (A) back to the χ spheres at $T_1$ and $T_2$, respectively, relates the waves in the crystal to the beams outside. The points $O_f$ and $G_f$ are what you record on the photographic film.

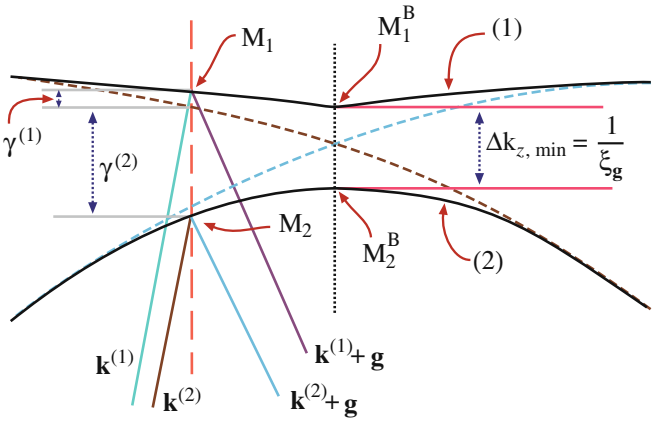


**FIGURE 15.5.** An enlarged region of Figure 15.4A showing how the vectors $\mathbf{k}^{(1)}$ and $\mathbf{k}^{(2)}$ are related to the quantities $\gamma^{(1)}$ and $\gamma^{(2)}$ and the distance $\Delta k_z$.

First, we need to know which points on the dispersion surface will actually correspond to the diffraction condition we have chosen. We also need to know the orientation of the specimen relative to the beam and the orientation of the Bragg planes (which is why we start by fixing this).

*To begin*. We consider the case where the surface of the specimen is parallel to **g**; we will explain why we are so specific on this point in a moment.

Now we have fixed the specimen and **g** relative to the optic axis. Next we orient the incident beam. Note that the beam is not parallel to the (*hkl*) planes; its $\mathbf{k}_1$ is determined by $\boldsymbol{\chi}$ but isn't shown in the figure. We will excite points $M_1^B$ and $M_2^B$ on separate branches of the dispersion surface because this is where the dotted line cuts the two surfaces. The extinction distance will then correspond to $\Delta k^{-1}$ for $s = 0$ as in Section 13.10. If we now tilt the incident beam so that $\boldsymbol{\chi}$ moves closer to the vertical (keeping the specimen fixed), then the excited points become $M_1$, and $M_2$ and, as we see in Figure 15.4, $s$ becomes negative.

We define the lines $M_1^B M_2^B$ and $M_1M_2$ to be *tie lines* because they tie together points on the different branches of the dispersion surface. Both tie lines are parallel to the BZB because we chose the top surface of the specimen to be parallel to **g**.

Each of these tie lines is normal to the surface that produces it.

The diagrams of the dispersion surface in Figures 15.4 and 15.5 contain lots of reminders

- For this orientation, $\mathbf{k}_x$ is the same for all **k** vectors ending on O.
- You can recognize $\gamma^{(1)}$ and $\gamma^{(2)}$ from Section 13.7.
- The vacuum wave vector $\boldsymbol{\chi}$ is always shorter than **K** or **k**.

We can understand these changes from the following argument. The O beam is always excited so $C_0^{(1)}$ and $C_0^{(j)}$ will always be relatively large. Which other values of $C$ are large will depend on where the Ewald sphere cuts the systematic row of relrods.

Now we can consider what happens when the surface of the specimen is *not* parallel to **g**. Here, the normal to the surface, **n**, is not parallel to the BZB (since the BZB is normal to **g**). However, the tie line is always parallel to **n** so the tie line is no longer parallel to the BZB. Remember: this construction is graphically matching the components of the **k** vector which are parallel to the surface of the specimen. We saw this clearly in Figure 15.4 where we commented that $\mathbf{k}_x$ is the same for all the vectors ending on O because we chose **g** to be parallel to the surface and the surface to be normal to the optic axis in that case.

We don't need tie lines in solid-state physics if the electrons are always moving in a perfect lattice where we don't consider surfaces.

**TIE LINES**

The tie line is a graphical method of satisfying the boundary conditions imposed by the TEM specimen.

We are now ready to consider the more common TEM wedge specimen shown in Figure 15.6A and then we'll see how these excited Bloch waves relate to the DP.

In this figure we have drawn the wedge with the top surface horizontal. Thus we have tie line $\mathbf{n}_1$ along the optic axis. When the electrons exit the crystal at the inclined bottom surface, we again match components parallel to this surface so we have tie line $\mathbf{n}_2$. Notice that we must draw $\mathbf{n}_2$ through both $M_1$ and $M_2$. These tie lines don't excite extra points on the dispersion surface because we are leaving the crystal.

Once we're outside the crystal, we know that the wave vector must be $\boldsymbol{\chi}$ and that $\boldsymbol{\chi}$ defines a pair of spheres centered on O and G. So we extend the $\mathbf{n}_2$ tie lines until they reach the $\boldsymbol{\chi}$ spheres. Now we have excited four points, as we see graphically in Figure 15.6A. The points on the O circle are labeled $O_1$ and $O_2$; those on the G circle are $D_1$ and $D_2$. We have labeled the subscripts this way because they correspond to the plane waves $\boldsymbol{\chi}_0^{(1)}$, $\boldsymbol{\chi}_0^{(2)}$, etc., as also shown in Figure 15.6A.

*To conclude*. Now we have reached the final step. We have to relate these beams to the DP. Yes, they are real beams, not Bloch waves, because we are now outside the specimen and in a vacuum. We show this in Figure 15.6B. All of the $\boldsymbol{\chi}$ beams have been related to point $O_1$ because $\boldsymbol{\chi}_0^{(1)}$ is the incident beam. Remember: $\boldsymbol{\chi}_0^{(1)}$ is not vertical because we made **g** horizontal and tilted the incident beam. The vectors $\boldsymbol{\chi}_0^{(1)}$ and $\boldsymbol{\chi}_0^{(2)}$ are not quite parallel because although they are both radii of the same sphere of radius $\chi$, they actually originate at different points on the circle (see Figure 15.6A).

The conclusion is that we will have two spots at O and two spots at G. In other words, the fact that we have

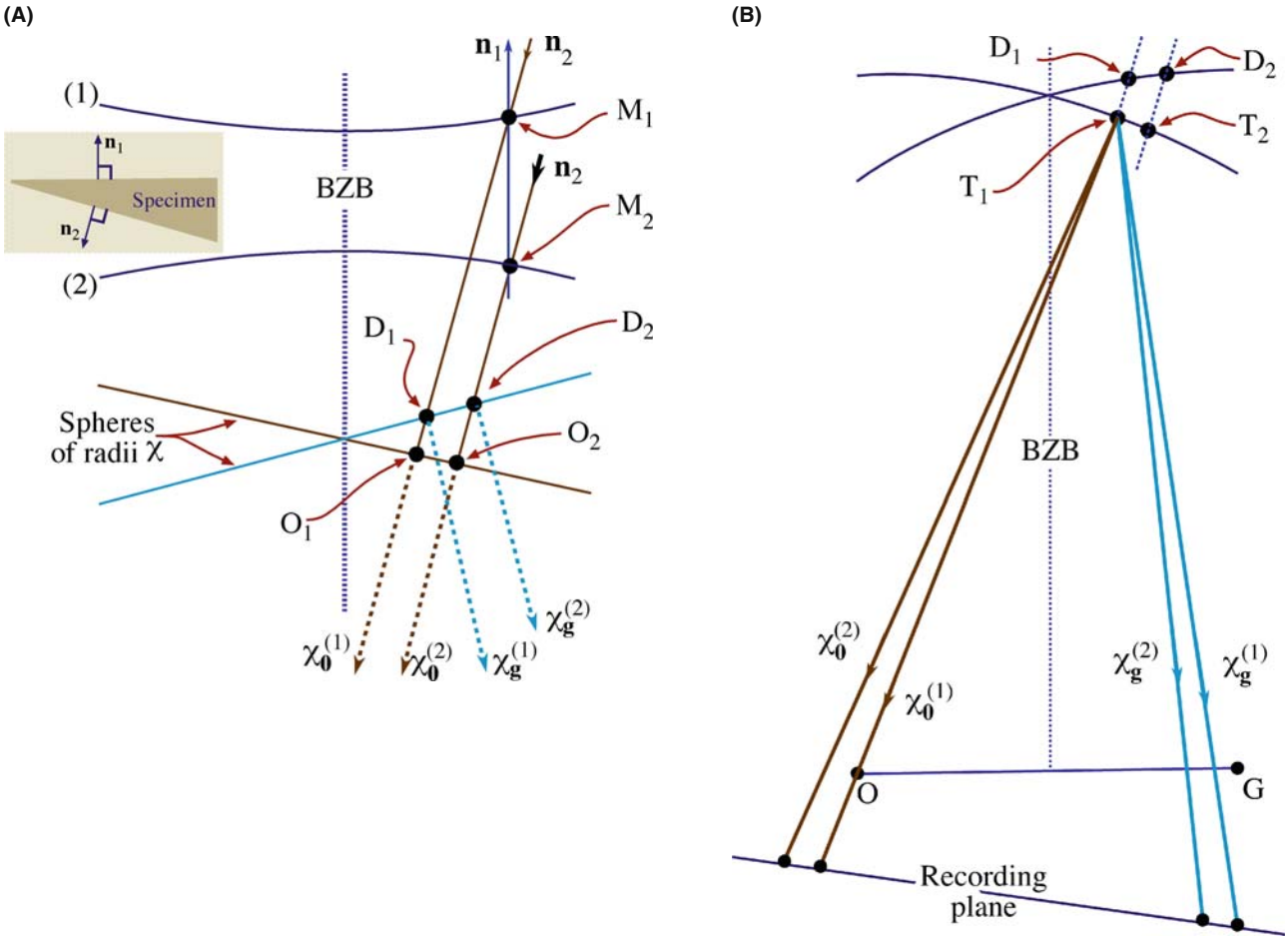


**FIGURE 15.6.** (A) The same diagram as Figure 15.4B, but for a wedge specimen with the top surface parallel to **g** (normal $\mathbf{n}_1$) and the bottom surface normal $\mathbf{n}_2$. Instead of exciting two points, $O_1$ and $O_2$, we excite two more, $D_1$ and $D_2$, which correspond to the plane waves $\chi_0^{(1)}$, $\chi_0^{(2)}$, outside the crystal. In (B) we relate all the beams to the point $O_1$ and we produce two beams at O and two at G. Thus we can predict that a wedge foil will give doublets at O and G.

a wedge specimen has split the spots at G. We will see these split spots in Chapter 18 and we will return to this topic in Chapter 23 when we discuss images.

It can be useful to extend the wedge case to the double wedge. For example, imagine an inclined planar defect in a parallel-sided slab with **g** parallel to the slab surface as shown in Figure 15.7. Everything is as before at the top surface. At the inclined interface then, tie lines do create new excited points $B_1$ and $B_2$ on the 1 and 2 branches of the dispersion surface.

Now, $\mathbf{n}_3$ is the tie line due to the bottom surface and $\mathbf{n}_3$ is parallel to $\mathbf{n}_1$. We extend the $\mathbf{n}_3$ tie lines to the $\chi$ spheres and find that now we have three $\chi_0$ vectors and three $\chi_D$ vectors. Translating these $\chi$ vectors to $O_1$ as the common origin produces the beam diagram shown in Figure 15.7B. Now we have three spots at O and three spots at G. We will return to this topic in Chapter 24 when we discuss images of planar defects, but here let's summarize the new concepts they give us

- The dispersion surface is a graphical approach to thinking about Bloch waves.
- We have to match the components of any wave entering and leaving any surface, internal or external.
- We use the exit-surface tie line to link to the $\chi$ spheres.
- Having two inclined surfaces causes a splitting of the Bragg beams.
- An internal interface, such as a stacking fault, increases the number of points excited on the dispersion surfaces and the number of spots at reflection G!

To understand the importance of these ideas, try to imagine what will happen when a defect, which is not abrupt, is present in the crystal (more on this in Section 15.8).

## 15.5 THE RELATION BETWEEN $U_g$, $\xi_g$, AND $s_g$

We can best appreciate the importance of the dispersion-surface construction by looking at Figure 15.4. This figure shows the original spheres as dashed lines: they are nearly flat close to the BZB. The electron beam is

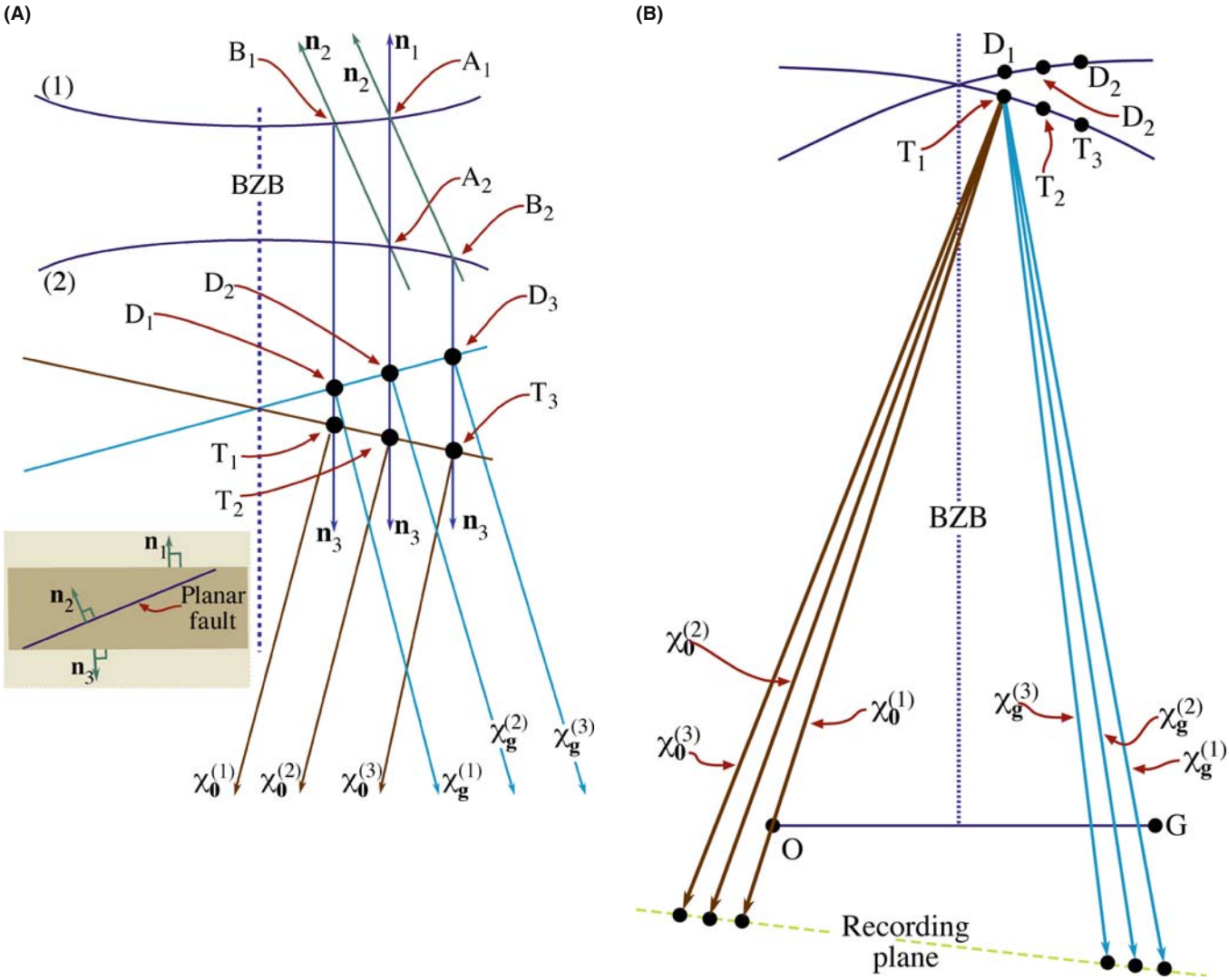


**FIGURE 15.7.** (A) An enlarged view of the dispersion surface in Figure 15.6 close to the BZB, but this time for a specimen in which both surfaces are parallel to **g** but there is an inclined fault which produces a third wave $\chi_0^{(3)}$ and $\chi_g^{(3)}$. If we then move all the vectors to $O_1$ again, we predict there will be three spots at O and three at G.

initially traveling with wave vector $\chi$ outside the crystal. When the beam enters the crystal the $z$ component of this wave vector changes (this is the refraction effect we saw in Chapters 11 and 13), but the $xy$ component is unchanged. Therefore, the allowed **k** vectors in the crystal are $\mathbf{k}^{(1)}$ and $\mathbf{k}^{(2)}$. One **k** vector begins on branch 1 and ends at O, while the other begins at branch 2 and ends at O.

**BRANCHES AND BEAMS**

There are only two **k** vectors because there are only two branches of the dispersion surface. There are two branches of the dispersion surface because we have a crystal potential (hence $U_\mathbf{g}$). There are only two branches because we are considering only two beams.

Clearly we can draw in $\mathbf{k}_g^{(2)}$ and $\mathbf{k}_g^{(1)}$ by adding **g**. Now, how does $\mathbf{k}_0^{(1)}$, say, relate to **K**? The point K is also determined by the tie line through $\boldsymbol{\chi}$, and lies on the circle centered on O. Most importantly, neither $\mathbf{k}_1$ nor $\mathbf{k}_2$ is equal to **K**. If you look back at equation 13.41 you can see that

$$k_z^{(i)} - K_z = \gamma^{(i)} \tag{15.8}$$

So $\gamma^{(i)}$ is simply the distance of the point $M_j$ from the $K$ sphere centered on O. We can write this relationship explicitly

$$\mathbf{k}^{(i)} = \mathbf{k}_z^{(i)} + \mathbf{k}_x^{(i)} \tag{15.9}$$

$$= \left(K + \gamma^{(i)}\right)\mathbf{u}_z + k_x\mathbf{u}_x \tag{15.10}$$

Notice that the last term here is independent of $i$. Look again at Figure 15.4. We can see that $\Delta k_z$ is a minimum when $M_1$ and $M_2$ lie on the BZB. In that situation

$$\Delta k_{z_{\min}} = \gamma^{(1)} - \gamma^{(2)} \tag{15.11}$$

Simply by looking at the diagram, and as expected from Chapter 13, you also know that

$$\gamma^{(1)} - \gamma^{(2)} = \frac{U_{\mathbf{g}}}{k} = \frac{1}{\xi_{\mathbf{g}}} \tag{15.12}$$

So

$$\Delta k_z = \frac{1}{\xi_{\mathbf{g}}} \tag{15.13}$$

The origin of the thickness oscillations that we will see in the two-beam TEM image is the difference in wavelength of the two Bloch waves. It's the beating between the two Bloch waves.

Thus we see that the gap $\Delta k_z$ at the BZB is given by the reciprocal of the extinction distance. We'll summarize again to be quite sure that it is clear!

- We have a crystal, therefore $U_{\mathbf{g}} \neq 0$.
- Since $U_{\mathbf{g}} \neq 0$ we have two branches to the dispersion surface and hence a band gap.
- The bandgap is $\Delta k_z$.
- Hence we have a finite extinction distance (i.e., $\xi_{\mathbf{g}}$ is not infinite).

An aside: think how $s_{\text{eff}}$ and $s$ would be related if $\xi_{\mathbf{g}}$ were infinite. (Go back to equation 13.47.)

If the tie line $M_1M_2$ does not lie on the BZB then when we draw the Ewald sphere centered just below $M_1$ (with radius of length $1/\lambda$ or $|K|$) we see that $s_{\mathbf{g}}$ is nonzero. We can easily see from the equations in Section 13.10 that, in general, $\Delta k_z$ is given by

$$\Delta k_z = s_{\text{eff}} = \frac{1}{\xi_{\text{eff}}} \tag{15.14}$$

This equation is the key to understanding the origins of the extinction distance and why the effective extinction distance depends on the size of the excitation error, **s**. It says that the band gap increases as we increase **s**. Looking at it another way, as we move the tie line off the BZB, the band gap $\Delta\mathbf{k}$ increases.

Some questions raised here are

- What is the physical reason that $\Delta k_z$ is related to **s**?
- What happens if **g** is not parallel to the foil surface or, indeed, if the foil surfaces are not parallel to one another?

You can also appreciate why we had a problem defining **s** when we first encountered it!

## 15.6 THE AMPLITUDES OF BLOCH WAVES

In Section 13.9, we found that the total wave function for the two-beam case can be expressed as the sum of two Bloch waves

$$\psi(\mathbf{r}) = \mathcal{A}^{(1)}b^{(1)} + \mathcal{A}^{(2)}b^{(2)} \tag{15.15}$$

We showed that the relative contributions of the two Bloch waves $\mathcal{A}^{(1)}$ and $\mathcal{A}^{(2)}$ are $\cos\beta/2$ and $\sin\beta/2$, respectively; in addition, $w = \cot\beta = s\xi_{\mathbf{g}}$.

We also showed in Section 13.8 that

$$b^{(1)}\left(\mathbf{k}^{(1)}, \mathbf{r}\right) = C_{\mathbf{0}}^{(1)} e^{2\pi i \mathbf{k}^{(1)} \cdot \mathbf{r}} + C_{\mathbf{g}}^{(1)} e^{2\pi i \left(\mathbf{k}^{(1)} + \mathbf{g}\right) \cdot \mathbf{r}} \tag{15.16}$$

and

$$b^{(2)}\left(\mathbf{k}^{(2)}, \mathbf{r}\right) = C_{\mathbf{0}}^{(2)} e^{2\pi i \mathbf{k}^{(2)} \cdot \mathbf{r}} + C_{\mathbf{g}}^{(2)} e^{2\pi i \left(\mathbf{k}^{(2)} + \mathbf{g}\right) \cdot \mathbf{r}} \tag{15.17}$$

The Bloch wave coefficients were given by equation set 13.31

| $C_0^{(1)}$ | $C_0^{(2)}$ | $C_g^{(1)}$ | $C_g^{(2)}$ |
|---|---|---|---|
| $\cos\beta/2$ | $\sin\beta/2$ | $-\sin\beta/2$ | $\cos\beta/2$ |

Now we can consider some special cases and examine the actual values for $C_{\mathbf{0}}^{(1)}$, $\mathcal{A}^{(1)}$, etc. (Table 15.1).

For the Bragg case, $s_{\mathbf{g}} = 0$, **g** is exactly excited and $\mathcal{A}^{(1)}$ and $\mathcal{A}^{(2)}$ are both equal to $1/\sqrt{2}$. In other words, the two Bloch waves are equally excited.

For the case where $s_{\mathbf{g}} < 0$, we now have $\cos(\beta/2) > \sin(\beta/2)$ so that $\mathcal{A}^{(1)}$ is greater than $\mathcal{A}^{(2)}$. If we reverse the sign of $s$, $\cos(\beta/2) < \sin(\beta/2)$ and $\mathcal{A}^{(1)}$ is less than $\mathcal{A}^{(2)}$.

**TABLE 15.1 Values of Bloch Wave Variables**

| $s$ | $w$ | $\beta$ | $\beta/2$ | $\cos(\beta/2)$ | $\sin(\beta/2)$ |
|---|---|---|---|---|---|
| 0 | 0 | $\pi/2$ | $\pi/4$ | $1/\sqrt{2}$ | $1/\sqrt{2}$ |
| +0.01 | $+\Delta$ | $(\pi/2)-\delta$ | $(\pi/4)-(\delta/2)$ | $(1/\sqrt{2})+\epsilon$ | $(1/\sqrt{2})-\epsilon$ |
| −0.01 | $-\Delta$ | $(\pi/2)+\delta$ | $(\pi/4)-(\delta/4)$ | $(1/\sqrt{2})-\epsilon$ | $(1/\sqrt{2})+\epsilon$ |

**AMPLITUDE OF BLOCH WAVE**

Whether Bloch wave 1 or Bloch wave 2 has the largest amplitude depends on the sign of s.

Now, let's relate this information to the dispersion surface shown in Figure 15.4. When $s_{\mathbf{g}} < 0$, as shown here, the $M_1M_2$ tie line is to the left of the BZB, which

is associated with reflection G. When the tie line is closer to O than G, Bloch wave 1 is more strongly excited; the reverse is true when the tie line crosses the BZB. We should remember that the analysis in Chapter 13 was for a two-beam case, where we were close to the Bragg condition. So this discussion of $\mathcal{A}^{(1)}$ and $\mathcal{A}^{(2)}$ only applies to small values of **s**.

## 15.7 EXTENDING TO MORE BEAMS

If we allow more beams to contribute to the image, we can imagine the dispersion surface for the case where $U_{\mathbf{g}} = 0$ by constructing more spheres, shown in Figure 15.8. If we have $n$ beams then we will have $n$ spheres. Note that each sphere is centered on its corresponding reciprocal-lattice point and neighboring spheres intersect periodically spaced BZBs. The gap in Figure 15.3 always occurs at the BZB. The BZB itself always corresponds to a plane which is the perpendicular bisector of a **g** vector. Thus the diagram for >2 beams shown in Figure 15.8 will become more complicated with many band gaps and many branches as shown in Figure 15.9. The magnitude of the band gap does decrease as the rank of the neighboring branches increases.

In Chapter 27, we'll discuss what happens in images when 3**g** is excited. We will actually consider the two-beam condition where **0** and 3**g** are the two beams.

We follow the convention used by Metherell and number the branches of the dispersion surface from top down.

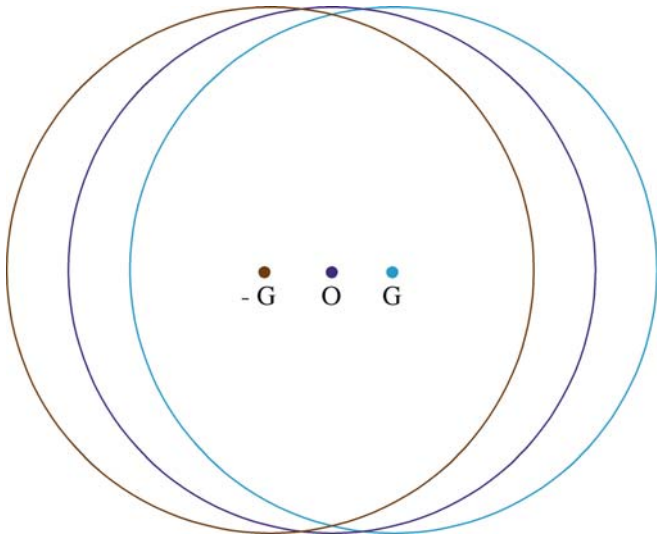


**FIGURE 15.8.** Three dispersion spheres due to three reflections, –G, O, and G. If we had $n$ spots we would have $n$ spheres.

Then $i = 1$ corresponds to the branch with the highest kinetic energy. Remember that all the electrons have the same total energy in this treatment. You must also be aware that some earlier texts number the top branch two and the second branch one, following Hirsch et al. This was fine when only two branches were considered.

We can still associate the amplitudes $C_{\mathbf{0}}$, $C_{\mathbf{g}}$, etc., with the sphere centered on **0**, **g**, etc. The result is shown by the labels $C_{\mathbf{0}}$, $C_{\mathbf{g}}$, etc., in Figure 15.9. For

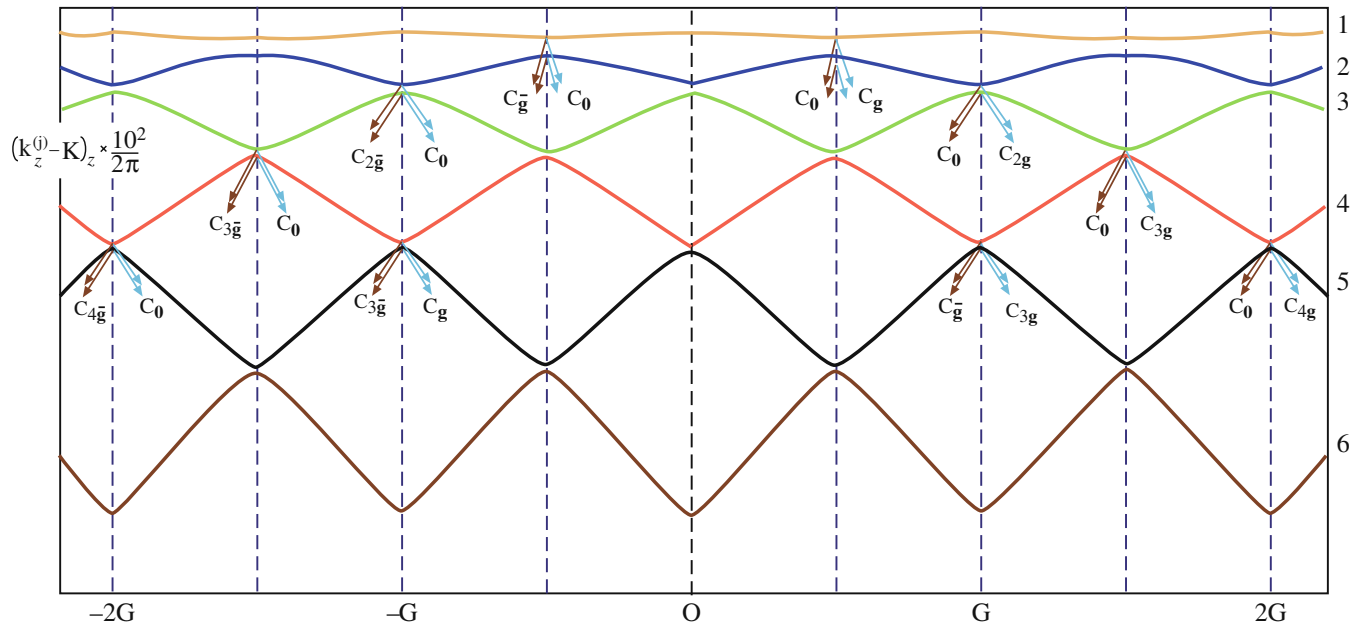


**FIGURE 15.9.** Six branches of the dispersion surfaces. The two branches $i = 1$ and $i = 2$ have the highest energy and give the largest band gap; notice that these branches give the terms in $C_{\mathbf{0}}$ and $C_{\mathbf{g}}$; smaller gaps occur between branches with lower energy. The diagram can be approximated to a set of spheres centered on O, ±G and ±2G, etc.; $C_{\mathbf{0}}$ is 'normal' to the sphere centered on O, while $C_{\mathbf{g}}$ is 'normal' to the sphere centered on **g**, etc.

example, imagine the original spheres centered on **0** and **g**; they intersect on the BZB which passes through **g**/2 so the $C_{\mathbf{0}}$, $C_{\mathbf{g}}$ are labeled as shown.

Similarly, the spheres centered on **0** and 3**g** intersect on the BZB which passes through 3**g**/2 so $C_{\mathbf{0}}$, $C_{3\mathbf{g}}$ are labeled. As a general rule, $C_{n\mathbf{g}}$ will be largest for the pair of reflections which are excited, i.e., **0** and $n$**g** and will be related by the $n$**g**/2 BZB.

We now extend these arguments to the situation where many beams are excited. Values of $C$ other than $C_{\mathbf{0}}$ and $C_{n\mathbf{g}}$ will be non-zero since it's no longer a two-beam case. So the tie line $M_1M_2$ will then intersect many branches of the dispersion surface. The reason these contributions are smaller when **g** is excited is that they do not intersect the **0** circle. However, they can contribute to the image. Figure 15.9 shows how this can be visualized. (Remember the dispersion surface is a way of visualizing Bloch wave coefficients.) If we satisfy reflection 2G, then $C_{\mathbf{0}}^{(1)}$, $C_{\mathbf{0}}^{(2)}$, $C_{2\mathbf{g}}^{(1)}$, and $C_{2\mathbf{g}}^{(2)}$ are all large. The gap $\Delta k_{4,5}$ between branch 4 and branch 5 at G (on the BZB) is small; the 'circles' would have intersected in the vacuum. If we think about the Ewald sphere we can show that the **s** values for $\bar{\mathbf{g}}$ and 3**g** are identical. We'll see later (Chapter 26) that these reflections will actually couple strongly, although both are weakly excited and the extinction distance is large (because the gap $\Delta k_{4-5}$ is small). The extinction distance for the coupling of $\bar{\mathbf{g}}$ and 3**g** when 2**g** is strongly excited is $\xi_{4\mathbf{g}}$ ($\xi_{3\mathbf{g}-(-\mathbf{g})}$). We can see this is true by looking at the branch 4/5 gap on the BZB for G.

## 15.8 DISPERSION SURFACES AND DEFECTS

The original reason for introducing the concept of Bloch waves was that only Bloch waves can exist in a periodic potential, i.e., there are no beams in the crystal. So what happens when a defect is present? We'll discuss this situation in some detail in Chapters 23–26 but will mention the basic ideas here, emphasizing the Bloch waves rather than the defects.

In Section 15.4, we discussed the effect that a planar fault can have on the Bloch waves using the dispersion-surface representation. What we were actually doing was matching the components parallel to the planar defect, so the effect of the planar fault was to create new tie lines $\mathbf{n}_2$. The general result is that, when a defect is present, energy is transferred from one Bloch wave to the other along the tie line; this is known as *interband scattering*. This concept is not only important for our understanding of images of planar defects but also illustrates a general principle for defects.

The difficulty with non-planar defects is that the tie lines are not so well defined. You can, however, imagine the result: instead of having points on the dispersion surface, we will have a distribution of points. We then relate this distribution to the DP. We do this with the tie lines normal to the exit surface and then translate to $O_1$ in the usual way. So, our distribution of points on the dispersion surface will become a distribution of spots in the DP; this distribution is what we will call a streak in Chapter 17.

## CHAPTER SUMMARY

Dispersion surfaces allow us to draw diagrams to represent the equations given in Chapter 14. These surfaces are essentially plots of the **k** vector of the Bloch waves (which is directly related to the energy) versus the **K** vector. They correspond directly to the band diagrams, which are used extensively to represent energy levels in semiconductors; the difference is that in semiconductors, we emphasize energy by plotting energy versus reciprocal-lattice vector (our **K** vector). The **k** vectors themselves vary because, although the total energy of each electron is a constant, the potential energy decreases when the electron is close to the nucleus, causing the kinetic energy to increase.

The most important equation for imaging theory is 15.14, which relates $\Delta k_z$, $s_{\text{eff}}$, and $\xi_{\text{eff}}$. Notice that $\Delta k_z$ is defined for two Bloch waves but is only small when the Bragg equation is nearly satisfied. This relationship links Bloch waves and Bragg beams. $\Delta k$ is non-zero because we have a crystal which produces a periodic potential. $\Delta k$ gives rise to thickness fringes and all thickness effects. Thus we see that thickness variations are due to the interference, or beating, of pairs of Bloch waves. As we increase $n$, $\xi_{\mathbf{g}}$ increases because the gap between the two relevant branches of the dispersion surface becomes narrower. Defects present in the crystal cause a mixing or coupling of the Bloch waves: they 'tie' the branches of the dispersion surface and cause interband scattering.

We've emphasized throughout this chapter that the dispersion surface is a pictorial representation of the **k** versus $K$ relationship. We'll close by quoting the result derived by Kato.

In any wave field, the direction of energy flow is along the normal to the surface of the dispersion surface. This result is equally valid for 'electron wave packets' and other waves. The physicist might say that the Poynting vector is normal to the dispersion surface.

Although there are many texts that discuss dispersion surfaces and band gaps in semiconductors, beware of the $2\pi/\lambda$ versus $1/\lambda$ problem since many of the texts are written by, and for, physicists. Defect analysis using Bloch waves has generally been the preserve of the physicist. However, there are some excellent programs available which use a Bloch-wave approach analysis.

We give the usual caveat: beware of black boxes. Metherell's article goes to greater depth than covered here. However, it has been an inspiration for much of this chapter and is highly recommended for advanced study. It is beautifully written and explained, but is certainly more advanced than our text. If you want to delve deeper into this topic, this is *the* article. Note that Metherell uses the $e^{ikr}$ notation.

## REFERENCES

As in Chapter 14 we follow the treatment of Hirsch et al. as extended and illustrated by Metherell. For anyone familiar with Mathematica™ (or the corresponding) MatLab it would be an interesting challenge to construct (and share) notebooks for these diagrams.

## BLOCH WAVES


Ashcroft, NW and Mermin, ND 1976 *Solid State Physics* W.B. Saunders Co. Philadelphia. Chapter 8 ($2\pi/\lambda$ is used).

Kato, N 1957 *The Flow of X-rays and Materials Waves in Ideally Perfect Single Crystals* Acta Cryst. **11** 885–887.

Kittel, CJ 2004 *Solid-State Physics* 8th Ed. John Wiley & Sons New York.

Metherell, AJF 1975 in *Electron Microscopy in Materials Science* **II** 397–552 Eds. U Valdré and E Ruedl CEC Brussels. *The reference*.


## THE COMPANION TEXT

The companion text doesn't extend this topic much, but there is hope to have a discussion of the use of Mathematica™ notebooks in the future.

## SELF-ASSESSMENT QUESTIONS

Q15.1 What does the word dispersion mean in the context of this chapter?

Q15.2 Write down an expression for $b^{(j)}(\mathbf{r})$ in terms of $\mathbf{k}^{(j)}$ and $C_{\mathbf{g}}{}^{(j)}$.

Q15.3 We restrict our discussion to the case where only reflections in the ZOLZ are excited. What is the simple physical reason for doing this?

Q15.4 Draw the dispersion surface diagram for the two-beam case where the crystal has zero inner potential; then explain the term 'dispersion surface.'

Q15.5 The vectors $\mathbf{k}^{(1)}$ and $\mathbf{k}^{(2)}$ are not parallel to one another. What is the physical reason for this and does it have any implications?

Q15.6 Why do $\mathbf{k}^{(1)}$ and $\mathbf{k}^{(2)}$ end (or begin) on branches (1) and (2) and not on the 'curves' x and y?

Q15.7 We used to have $\mathbf{K}_D$. Now we have $\mathbf{k}^{(1)} + \mathbf{g}$ and $\mathbf{k}^{(2)} + \mathbf{g}$. Why don't we have $\mathbf{K}_D$? Does $\mathbf{K}_D$ still exist?

Q15.8 What is a BZB? Write out the name and explain what causes it.

Q15.9 Draw the dispersion surface for two beams where $\mathbf{g}$ is not satisfied. (Draw Figure 15.4 without looking at it).

Q15.10 Consider Figure 15.4 when the incident beam, $\boldsymbol{\chi}_1$, is parallel to the diffracting planes. Why is this not a good example of two-beam diffraction?

Q15.11 In Figure 15.4, M is 'below' the dispersion surface. Can it be above this surface? Justify your answer.

Q15.12 In Figure 15.4, $\mathbf{k}^{(2)} + \mathbf{g}$ is longer than $\mathbf{k}^{(2)} + \mathbf{g}$. Does this mean that $\lambda$ has changed?

Q15.13 In Figure 15.4, why is the tie line $M_1M_2$ normal to $\mathbf{g}$?

Q15.14 The wave vector $\boldsymbol{\chi}$ is always shorter than $\mathbf{K}$ or $\mathbf{k}$. Explain why this is so.

Q15.15 The tie line is a graphical method of satisfying the boundary conditions imposed by the specimen. Explain why this is so.

Q15.16 In Figure 15.6, are points $O_1$, $O_2$, $D_1$, and $D_2$ really relevant since they don't lie on the dispersion surface for the crystal?

Q15.17 Explain in words why there are three $\boldsymbol{\chi}_0$ vectors ($\boldsymbol{\chi}_0{}^{(1)}$, $\boldsymbol{\chi}_0{}^{(2)}$, and $\boldsymbol{\chi}_0{}^{(3)}$) in Figure 15.7.

Q15.18 In the two-beam case when G is on the Ewald sphere, what are the magnitudes of the Bloch wave coefficients?

Q15.19 If $s_{\mathbf{g}}<0$, we can show that $\mathcal{A}^{(1)} > \mathcal{A}^{(2)}$. What does this mean physically?

## TEXT-SPECIFIC QUESTIONS

The following questions contain the manufacturers' warning label.

T15.1 Why are there two expressions for $C_{\mathbf{g}}^{(j)}/C_{\mathbf{0}}^{(j)}$ in equation 15.1?

T15.2 What is the physical reason that $\Delta k_z$ is related to $s$?

T15.3 If **g** is not parallel to the foil surface, how will the Bloch-wave construction change?

T15.4 If the two surfaces of the specimen are not parallel to one another, how will the Bloch-wave construction change?

T15.5 When the specimen is oriented so that G is on the Ewald sphere, we again have a situation like that shown in Figure 15.9; many beams are excited but one does have $s_{\mathbf{g}} = 0$. You form a BF image. How does the periodicity of the thickness fringes relate to this diagram? In particular, how is the extinction distance related to the two-beam value?

T15.6 When the specimen is oriented with the beam parallel to the diffracting planes, we have a situation like that shown in Figure 15.9; many beams are excited but none have $s_{\mathbf{g}} = 0$. You form a BF image. How does the periodicity of the thickness fringes relate to this diagram?

T15.7 We initially follow Metherell's simplification of assuming that only reflections in the ZOLZ are excited. Discuss what complications might arise if we did not make this assumption. Are we likely to encounter this in practice, and if so, under what conditions?

T15.8 We also made the approximation that the accelerating voltage is high. Discuss when this approximation might break down.

T15.9 In Figure 15.4, we draw OG so that it is not parallel to $O_fG_f$. Could this really happen? Discuss why $T_1G_f$ is parallel to $T_2G$ and should this be so?

T15.10 In Figure 15.6B, why is $\chi_0^{(2)}$ not parallel to $\chi_0^{(1)}$ and why are there two such vectors when we are outside the crystal? What is the relevance of $D_2$ and $T_3$ in this figure?